Engineering Science and Technology, an International Journal 19 (2016) 1919–1928

HOSTED BY

ELSEVIER

Contents lists available at ScienceDirect

Engineering Science and Technology, an International Journal

journal homepage: www.elsevier.com/locate/jestch

Full Length Article

# Chemical reaction and Soret effects on hydromagnetic micropolar fluid along a stretching sheet

S.R. Mishra [a,*], S. Baag [b], D.K. Mohapatra [a]

[a] Department of Mathematics, Siksha 'O' Anusandhan University, Odisha, Bhubaneswar 751030, India
[b] Department of Physics, College of Basic Sciences and Humanities, OUAT, Bhubaneswar, India

ARTICLE INFO

*Article history:*
Received 23 May 2016
Revised 6 July 2016
Accepted 26 July 2016
Available online 21 August 2016

*Keywords:*
MHD
Micropolar
Porous medium
Thermal radiation
Non-uniform heat source
Thermal diffusion
Chemical reaction

ABSTRACT

Free convection effects of a micropolar fluid along a stretching sheet embedded in a porous medium in the presence of a volumetric non-uniform heat source is investigated in the present paper. Thermal diffusion and first order chemical reaction are also considered in the present study to govern the flow characteristic. The generalization of the earlier studies centers round: (i) The magnetohydrodynamic flow is made to pass through a porous medium characterized by a non-Darcian drag coefficient affecting the momentum equation. (ii) The energy equation is modified with the interplay of non-uniform heat source. (iii) Consideration of chemically reactive species characterized by first order chemical reaction and thermal diffusion i.e. Soret modifying the equation of species concentration. Similarity transformation technique is used to transform the governing nonlinear partial differential equations into ordinary differential equations. The numerical solutions are achieved showing the effects of pertinent parameters. For verification of the present findings the results of this study have been compared with the earlier works in particular cases.



## 1. Introduction

In recent years, the theory of micropolar fluid has attracted significant attention among the researchers. Moreover, micropolar fluids could be able to model the fluid in the presence of dust particle. The presence of micropolar fluid can be found in polymer fluids, animal blood, fluids suspensions etc. Further, micropolar fluids have numerous practical applications in engineering to heat and mass transfer area. Number of literatures is available on the thermal boundary layer flows over moving boundaries [1,2]. Pioneering work in the field of micropolar fluids is initiated by Eringer [3]. Principally, micropolar fluids consisted with different class of fluid microstructure and non-symmetrical stress term.

Sakiadis [4] studied the behavior of laminar boundary layer on continuous solid surfaces. The mathematical problem was solved by using two different methods and the results are in good agreement between two methods of solution. Kim and Lee [5] studied the problem of the MHD oscillatory flow of a micropolar fluid over a vertical porous plate. In their study, they considered electrically conducting oscillatory two dimensional laminar viscous incompressible flows. In order to simplify boundary conditions Kim and Lee [5] assumed that the size of holes in the porous medium was much bigger compare to the microscopic length scale. Chen and Char [6] studied the effect of heat transfer on a continuous stretching surface with suction or blowing. A power law variation of wall temperature was considered to a horizontal heated surface. Grubka and Bobba [7] investigated the influence of surface temperature change on continuous and linearly starching surface and then solved by using a series solution to the energy equation based on hypergeometric (Kummer's) functions. As a result, magnitude of the temperature parameter affects the direction and quantity of the heat flow. No heat transfer was observed between the continuous surface and the ambient at $\gamma < 0$, where $\gamma$ is the temperature parameter.

In recent years, several studies have been conducted on Darcy convective transport phenomena [8] such as geothermal reservoir, petroleum industry, thermal insulation, blood flow and artificial analysis. The direct numerical simulation of blood flow through curved geometry for different curvature has been studied to investigate the effect of Dean number and magnetic field [9–14]. In industrial aspect the quality of the products as well as the cost of the production depends on the speed of material collection and the heat transfer rate. Instead of porous medium the flow characteristic in presence of stretching sheet is a great interest to many researchers. Pioneering work in this area has been performed by

* Corresponding author.
*E-mail addresses:* satyaranjan_mshr@yahoo.co.in (S.R. Mishra), sbaag22@gmail.com (S. Baag).

Peer review under responsibility of Karabuk University.

http://dx.doi.org/10.1016/j.jestch.2016.07.016
2215-0986/

**Nomenclature**

| | |
|---|---|
| $A^*$, $B^*$ | coefficients of space and temperature dependent heat source/sink |
| $b$ | stretching parameter |
| $B_o$ | magnetic field of constant strength |
| $c_f$ | drag coefficient |
| $C_f$ | local skin friction coefficient |
| $c_p$ | specific heat |
| $C$ | concentration of the fluid |
| $C_w$ | stretching sheet concentration |
| $C_\infty$ | ambient concentration |
| $Ec$ | Eckert number |
| $F$ | inertia-coefficient |
| $g$ | microrotation profile |
| $j$ | reference length |
| $\Delta$ | material parameter |
| $Kp$ | porous parameter |
| $k_p^*$ | permeability of the porous medium |
| $k_f$ | thermal conductivity |
| $K$ | consistency coefficient |
| $M$ | magnetic parameter |
| $Nu_x$ | local Nusselt number |
| Pr | generalized Prandtl number |
| $q'''$ | non-uniform heat source/sink |
| $\mathrm{Re}_x$ | local Reynolds number |
| $s$ | surface condition parameter |
| $Sc$ | Schmidt number |
| $Kc$ | chemical reaction parameter |
| $T$ | temperature of the fluid |
| $T_w$ | stretching sheet temperature |
| $T_\infty$ | ambient temperature |
| $u_w$ | characteristic velocity |
| $u$ | velocity along the $x$-direction |
| $v$ | velocity along the $y$-direction |
| $x, y$ | coordinates |

*Greek symbols*

| | |
|---|---|
| $\alpha$ | space dependent heat source/sink parameter |
| $\beta$ | temperature dependent heat source/sink parameter |
| $\theta(\eta)$, $\phi(\eta)$ | non-dimensional temperature and concentration parameter |
| $\eta$ | similarity variable |
| $\upsilon$ | kinematic viscosity |
| $\tau$ | stress tensor |
| $\sigma$ | electrical conductivity of the fluid |
| $\rho$ | density of the fluid |
| $\gamma$ | spin gradient viscosity |
| $\varepsilon$ | porous parameter |
| $\tau_{xy}$ | shear stress component of the stress tensor |
| $\lambda_t$ | thermal buoyancy parameter |
| $\lambda_c$ | solutal buoyancy parameter |

Crane [15], who studied 2D boundary layer flow of an incompressible and viscous fluid. McCormack and Crane [16] discussed the physical characteristics of boundary layer flow over a stretching sheet, where the sheet is moving along its own plane direction. Mohanty et al. [17] analyzed heat and mass transfer effect of micropolar fluid over a stretching sheet. Mishra et al. [18] studied on magnetohydrodynamic free convection in a micropolar fluid with heat source.

MHD flow and heat transfer adjacent to a stretching vertical sheet is analyzed by Ishak et al. [19]. Mehmood et al. [20] studied an oblique stagnation flow of Jeffery fluid over a stretching convective surface: Optimal solution. Akbar et al. [21] studied numerical analysis of magnetic field on Eyring–Powell fluid flow towards a stretching sheet. Abel along with his co-authors [22] discussed the effects of space and temperature dependent heat source on viscoelastic fluid flow and heat transfer over a stretching sheet, while Qasim et al. [23] reported the effect of heat transfer in a micropolar fluid over a stretching sheet with Newtonian heating. Pal and Mondal [24] studied the effect of variable viscosity on MHD non-Darcy mixed convection heat transfer over a stretching sheet embedded in a porous medium with non-uniform heat source/sink. The well-known Forchheimer's extension technique was used to describe the governing flow in the porous medium. The nonlinear governing equations were solved numerically by using Runge–Kutta–Fehlberg method associated with shooting technique.

Bhukta et al. [25] have analyzed heat and mass transfer on MHD flow of a viscoelastic fluid through porous medium. Recently, Jeffrey fluid in the boundary layer is investigated over stretching sheet [26,27] by using Homotopy Analysis Method (HAM) and the flow, heat and mass transfer rate are controlled by using magnetic field. Many researchers have been studied the influence of transverse magnetic field on such type of fluids over a stretching sheet owing to some specific characteristic of magnetic field. Haq et al. [28] investigated that, radiation effect on stagnation point flow of micropolar nanofluid over a stretching surface. Recently, Baag et al. [29] studied the MHD flow of a viscoelastic fluid past between infinite parallel plates with time dependent suction. Further, many researchers [30,31] studied the heat and mass transfer effects on MHD flow over a stretching shhet. Tripathy et al. [32] analyzed the effect of first order chemical reaction effect on MHD free convective surface over a moving vertical plane. Hayat et al. [33] presented the slip flow effects on peristaltic transport in an inclined asymmetric channel with mass transfer and chemical reaction. Exact solution for peristaltic transport of micropolar fluid in a channel in the presence of heat source/sink was presented by Hayat et al. [34]. Further, Hayat et al. [35,36] analyzed thermal diffusion and diffusion-thermo effects in peristaltic transport of physiological fluids with chemical reaction: A mathematical analysis. Moreover, they [37] have studied MHD stagnation point flow of Jeffrey fluid over a convectively heated stretching sheet.

Kumar [38] has studied the dynamics of hydromagnetic micropolar flow along a stretching sheet. His work was confined to the flow within the regions i.e. velocity, thermal and concentration boundary layers. He has considered the mass transfer of species without chemical reaction. Further, the flow problem is considered in the absence of porous matrix in the study of Kumar [38]. Moreover, though he has considered the viscous dissipation and Joule dissipation effects in energy equation but not considered any volumetric heat source either constant or variable strength which are of usual occurrence.

Motivated by above literatures and application the present paper explores the free convective heat and mass transfer from a vertical plate embedded in electrically conductive micropolar fluid. As the literature is beset with stabilizing/destabilizing effect of heat source on the flows in boundary layer, the necessity of inclusion of heat source is warranted. Add to it, the mass transfer of non-reactive species of industrial fluid is a far reaching cry, and hence the justification of accounting for the chemical reaction arises. Therefore, the present study deals with a flow model of micropolar fluid with non-uniform heat source and first order chemical reaction. A nonlinear non- Darcy model is applied to account for the effect of porous matrix on the flow phenomena.

Secondly, non-uniform volume heat source/sink is introduced to the energy equation. Finally, a first order chemical reaction term has been added to concentration boundary layer to account for the effect of chemical reacting species.

Darcy's law usually assumed to be the fundamental equation [39,40] when a flow past through porous medium. The principle of Darcy's law is the velocity components are directly proportional to the gradient of pressure. Hence, this law is only valid for low speed flows. The force of the fluid which is also proportional to the velocity components may be deviated from the Darcy drag force [41]. Brinkman have proposed generalization considering the convective force. To study the flow embedded by porous medium the generalized Darcy law should be used. Moreover, as we have considered modified Darcy law which is to account for the dissipative terms such as viscous dissipations and Joule dissipation characterized by Eckert number ($Ec$) which does not depend upon purely physical property but it grows in proportion to the square of the velocity. Therefore, the present study aims at exploring the influences of the pertinent physical parameters relating to the aforesaid flow, heat and mass transfer dynamics in the presence of radiation and Soret number (Fig. 1).

## 2. Mathematical formulation

Consider an electrically conducting steady two dimensional incompressible micropolar fluid flow on a moving sheet. A magnetic field of intensity $B_0$ is perpendicularly applied to the stretching sheet. It is assumed that the effect of both magnetic and electric field is very less while magnetic Reynolds number of the flow is small. Let the $x$ axis represent the position of the sheet and $y$-axis perpendicular to it. The corresponding velocity components are $u$ and $v$ along $x$-axis and $y$-axis respectively and N is micro-rotation component. Also $T_w$ is the wall temperature of the sheet, $T_\infty$ is temperature of the fluid far away from the sheet and $T$ is temperature of the fluid in boundary layer. The governing equations of micropolar fluid following Kumar [38] with the appropriate boundary conditions are given by

$$\frac{\partial u}{\partial x}+\frac{\partial v}{\partial y}=0 \tag{1}$$

$$u\frac{\partial u}{\partial x}+v\frac{\partial u}{\partial y}=\left(\upsilon+\frac{k_v}{\rho}\right)\frac{\partial^2 u}{\partial y^2}+\frac{k_v}{\rho}\frac{\partial \omega}{\partial y}-\frac{\sigma B_0^2}{\rho}u-\frac{\upsilon}{k_p^*}u-\frac{c_f}{\sqrt{k_p^*}}u^2 + g\beta_T(T-T_\infty)+g\beta_C(C-C_\infty) \tag{2}$$

$$j\rho\left(u\frac{\partial \omega}{\partial x}+v\frac{\partial \omega}{\partial y}\right)=\gamma\frac{\partial^2 \omega}{\partial y^2}-k_v\left(2\omega+\frac{\partial u}{\partial y}\right) \tag{3}$$

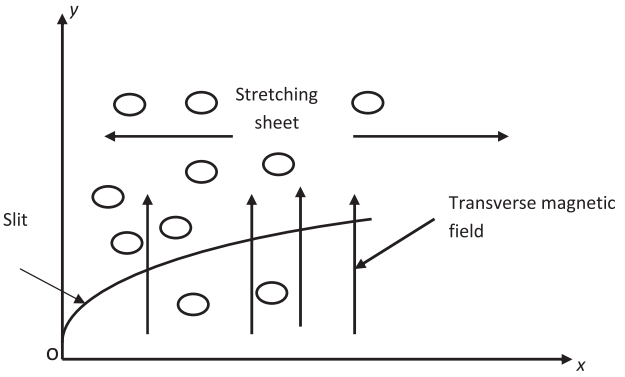


**Fig. 1.** Flow configuration.

$$\rho c_p\left(u\frac{\partial T}{\partial x}+v\frac{\partial T}{\partial y}\right)=\frac{\partial}{\partial y}\left(k_f\frac{\partial T}{\partial y}\right)+(\mu+k_v)\left(\frac{\partial u}{\partial y}\right)^2+\rho B_0^2u^2 + \frac{16\sigma^* T_\infty^3}{k_1}\left(\frac{\partial^2 T}{\partial y^2}\right)+q''' \tag{4}$$

$$u\frac{\partial C}{\partial x}+v\frac{\partial C}{\partial y}=D_m\frac{\partial^2 C}{\partial y^2}+\frac{D_m k_T}{T_m}\frac{\partial^2 T}{\partial y^2}-Kc(C-C_\infty) \tag{5}$$

$$\left.\begin{aligned} u=u_w=bx,\quad v=0,\quad \omega=-s\tfrac{\partial u}{\partial y},\quad T=T_w,\quad C=C_w,\quad at\ y=0\\ u=0,\quad \omega=0,\quad T=T_\infty,\quad C=C_\infty,\quad as\ y\to\infty\end{aligned}\right\} \tag{6}$$

The fourth and fifth terms on the right hand side of Eq. (2) contribute due to non-Darcian flow over porous media. The second term in Eq. (5) represents the first order chemical reaction. Following the work of Rees and Pop [42], it is assumed that $\gamma=(\mu+\frac{k_v}{2})j$, where $j=\frac{\upsilon}{b}$ as a reference length. The non-uniform heat source/sink $q'''$ is considered following [43]

$$q'''=\frac{\rho k_f u_w(x)}{x\mu}\left[A^*(T_w-T_\infty)f'+(T-T_\infty)B^*\right] \tag{7}$$

Here it is worth to note that the internal heat generation/absorption corresponds to $A^*>0$, $B^*>0$, $A^*>0$, $B^*>0$ respectively. The similarity transformations and dimensional variables have been used to transform Eqs. (2)–(5) into a set of ordinary differential equations. i.e.

$$\left.\begin{aligned} \xi=\left(\sqrt{\tfrac{b}{\upsilon}}\right)y,\quad u=bxf'(\xi),\quad v=-\sqrt{b\upsilon}f(\xi)\\ \omega=\sqrt{\tfrac{b^3}{\upsilon}}xg(\xi),\quad \theta(\xi)=\tfrac{T-T_\infty}{T_w-T_\infty},\quad \phi(\xi)=\tfrac{C-C_\infty}{C_w-C_\infty}\end{aligned}\right\} \tag{8}$$

In view of Eq. (8), the Eqs. (2)–(5) and the boundary conditions (6) are reduced to

$$(1+\Delta)f'''+ff''-(1+F)f'^2+\Delta g'-(M+Kp)f'+\lambda_t\theta+\lambda_c\phi=0 \tag{9}$$

$$\left(1+\frac{\Delta}{2}\right)g''+fg'-gf'-\Delta(2g+f'')=0 \tag{10}$$

$$\frac{(1+R+\varepsilon\theta)}{\Pr}\theta''+f\theta'-2f'\theta+(1+\Delta)Ecf''^2+EcMf'^2 + (1+\varepsilon\theta)(\alpha f'+\beta\theta)=0 \tag{11}$$

$$\phi''+Sc(f\phi'-2f'\phi)+ScS_0\theta''-Sc\delta\phi=0 \tag{12}$$

and the boundary conditions are

$$\left.\begin{aligned} f(0)=0,\quad f'(0)=1,\quad g(0)=-sf''(0),\quad \theta(0)=1,\quad \phi(0)=1,\\ f'(\infty)=0,\quad g(\infty)=0,\quad \theta(\infty)=0,\quad \phi(\infty)=0\end{aligned}\right\} \tag{13}$$

where the suffix prime denotes the order of differentiation with respect to $\xi$ and the dimensionless parameter are

$$\left.\begin{aligned} \Delta=\tfrac{k_v}{\mu},M=\tfrac{\sigma B_0^2}{\rho b},\Pr=\tfrac{\rho\upsilon c_p}{k_f},Ec=\tfrac{u_w^2}{c_p(T_w-T_\infty)},Sc=\tfrac{\upsilon}{D},\lambda_t=\tfrac{g\beta_T(T-T_\infty)}{b^2l},\alpha=\tfrac{k_fA^*}{Kc_p}\\ \lambda_c=\tfrac{g\beta_C(C-C_\infty)}{b^2l},F=\tfrac{c_fx}{\sqrt{k_p^*}},\tfrac{1}{Kp}=\tfrac{\upsilon}{bk_p^*},R=\tfrac{16T_\infty^3\sigma^*}{k_1k_f},S_0=\tfrac{k_T(T_w-T_\infty)}{T_m(C_w-C_\infty)},\delta=\tfrac{Kc}{b\upsilon},\beta=\tfrac{k_fB^*}{Kc_p}\end{aligned}\right\}$$

## 3. Physical quantities of interest

The shear stress can be written as:

$$\tau_w = \left[(\mu + k_v)\left(\frac{\partial u}{\partial y}\right) + k_v\omega\right]_{y=0} = (\mu + k_v)bx\sqrt{\frac{b}{\upsilon}}f''(0) \tag{14}$$

The local skin friction coefficient $C_f$ can be defined as

$$C_f = \frac{\tau_w}{(\rho u_w^2/2)} = \frac{(1+\Delta)f''(0)}{\sqrt{\mathrm{Re}_x}} \tag{15}$$

where $\mathrm{Re}_x = \frac{u_w x}{\upsilon}$ is the local Reynolds number and $u_w = bx$ as a characteristic velocity.

The couple stress at the surface is defined by

$$M_w = \left(\gamma\frac{\partial\omega}{\partial y}\right)_{y=0} = \mu u_w\left(1 + \frac{\Delta}{2}\right)g'(0) \tag{16}$$

The local surface heat flux $q_w(x)$, the local Nusselt number $Nu_x$, the local mass flux $j_w$ and Sherwood number $Sh_x$ are given as follows

$$q_w(x) = -k_f(T_w - T_\infty)\sqrt{\frac{b}{\upsilon}}\theta'(0) \tag{17}$$

$$Nu_x = \frac{xh(x)}{k_f} = -\sqrt{\frac{b}{\upsilon}}x\theta'(0) \Rightarrow \frac{Nu_x}{\sqrt{\mathrm{Re}_x}} = -\theta'(0) \tag{18}$$

$$j_w = -D\left(\frac{\partial C}{\partial y}\right)_{y=0} \tag{19}$$

$$Sh_x = \frac{j_w x}{D(C_w - C_\infty)} = -\sqrt{\frac{b}{\upsilon}}x\phi'(0) \Rightarrow \frac{Sh_x}{\sqrt{\mathrm{Re}_x}} = -\phi'(0) \tag{20}$$

## 4. Method of solution

In the present study, the robust Runge–Kutta method associated with shooting technique has been used to solved the couples non-linear Eqs. (9)–(12) subject to boundary conditions Eq. (13). The numerical solutions are obtained to exhibit the effects of emerging parameters on the velocity, temperature and concentration distributions through Figs. 2–12 and Tables 1–3 present the numerical computation of local skin friction, couple stress, Nusselt number and Sherwood number.

## 5. Results and discussion

Steady incompressible Hydromagnetic flow of micropolar fluid past over a stretching sheet embedded in a porous medium is considered in the present study. Momentum equation is enhanced with an addition of thermal and mass buoyancy, energy equation is associated with radiation and non-uniform heat source and the first order chemical reaction and thermal diffusion (Soret) are incorporated the mass transfer equation. The following discussion reveals the variation of different physical parameters which govern the flow, heat and mass transfer phenomena.

Fig. 2 exhibits the effect of magnetic parameter on the velocity, microrotation, temperature and concentration profiles in both the absence/presence of porous matrix. The curves I(blue),II(red) ($F = 0$, $Kp = 0$ and $M = 0, 1$) flow without porous medium represents the case of Kumar [38] in the absence of other emerging parameters characterizing the flow phenomena. It was observed that the present result is in good agreement with the previous work of Kumar [38]. From curves I(blue), II(red) and III(black), it is evident that all the parameters $M$ and $Kp$ reduce the velocity distribution. This reduction of velocity due to Lorentz force, a resistive force, produce electromagnetic origin, $M$ qualitatively agrees with desired result, causes a reduction along the main direction of flow. Whereas reverse trend is viewed in case of other three profiles such as microrotation, temperature and concentration. These profiles are enhanced as magnetic parameter increases in the absence/presence of porous matrix. Thus, it concluded that external body forces imposed due to magnetic field, porous medium and inertial coefficient favors the microrotation of the polar fluid.

The specialty of Fig. 3 is to bring out the effect of an important parameter $\Delta(=k_v/\mu)$, the material parameter which is the ratio of two viscosities of the fluid under consideration i.e. dynamic viscosity and vortex viscosity. For $\Delta = 1$ both the viscosities are of same order of magnitude. It is observed that the inclusion of material parameter $\Delta$ is to increase the velocity at all points in the absence of porous medium and the presence of porous matrix reduces it. It is clear to note that the microrotation profile reduces as $\Delta$ increases in the absence of porous matrix and the presence of porous matrix reduces it. Thus, it is concluded that effect of porosity of the medium combined with magnetic parameter gives rise to a

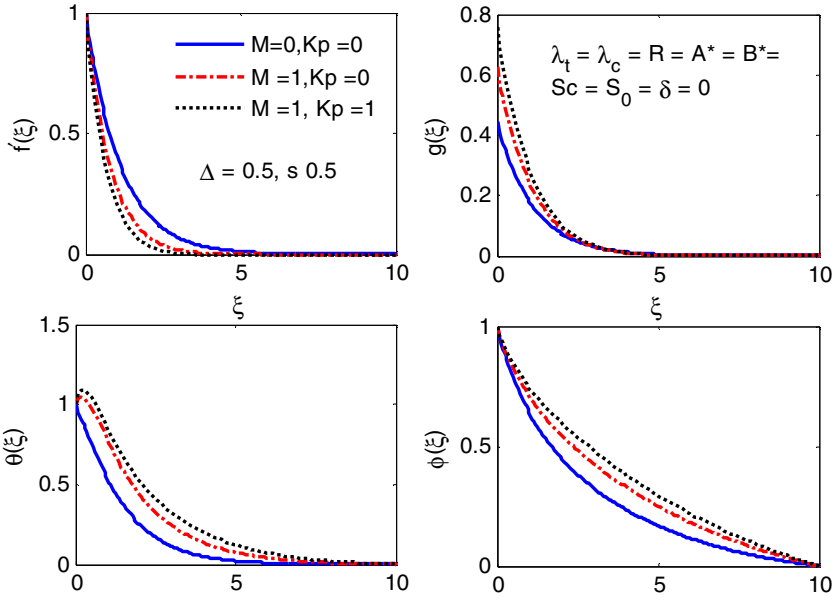


**Fig. 2.** Comparison plot for velocity, microrotation, temperature and concentration profiles.

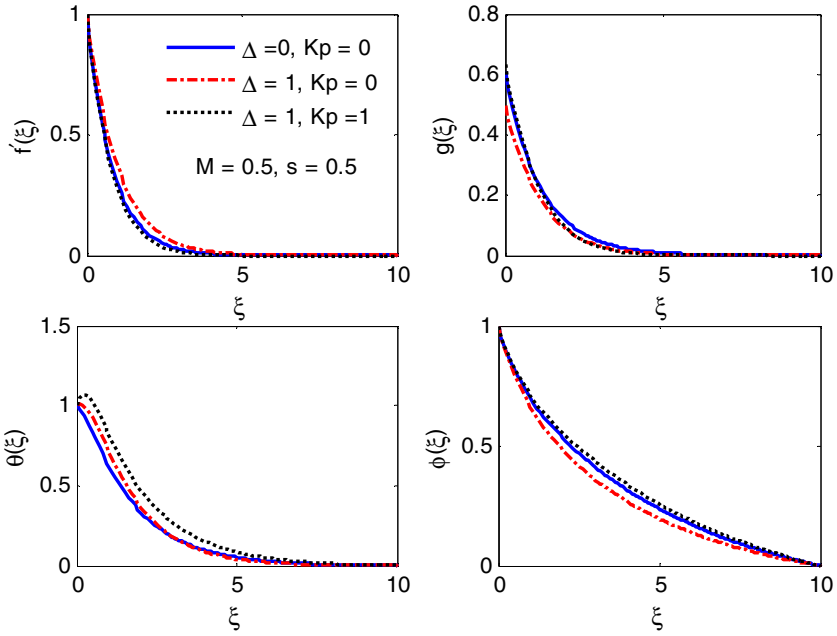


**Fig. 3.** Effects of Δ and *Kp* on velocity, microrotation, temperature and concentration profile.

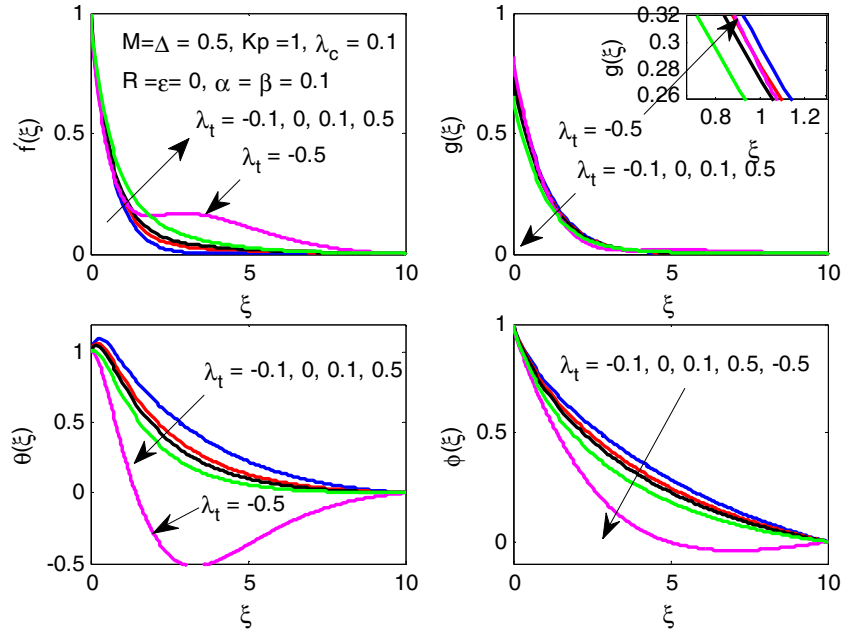


**Fig. 4.** Effect of $\lambda_t$ on velocity, microrotation, temperature and concentration profiles.

transverse compression producing a thinner boundary layer. The common characteristics of the profiles show that a rise of temperature is indicated near the boundary then temperature falls gradually to attend the ambient temperature within a few layers near the plate. It is to note that the material parameter $\Delta$ enhance the temperature in the thermal boundary layers. Thus, it is concluded that higher shear rate and viscous dissipation contribute to rise in temperature and hence favors the growth of thermal boundary layer. Further, in the absence of porous matrix the solutal concentration boundary layer reduces as material parameter increases whereas the presence of porous matrix enhances it.

Fig. 4 depicts the effect of thermal buoyancy parameter $\lambda_t$ on the flow phenomena. The positive value of $\lambda_t$ ($\lambda_t > 0$) corresponds to cooling of the plate and the negative value ($\lambda_t < 0$) corresponds to heating near the wall. It is clear to note that thermal buoyancy enhances the velocity distributions significantly whereas flow instability occurs for higher value of heating of the plate i.e. $\lambda_t = -0.5$ the velocity becomes higher at far of the plate. The microrotation profile has reverse trend for the increasing value of $\lambda_t$ but the distribution is insignificant. Further, the temperature and concentration profile retards significantly as $\lambda_t$ increases from negative values to positive i.e. $\lambda_t \geqslant -0.1$. It is interesting to note that for $\lambda_t = -0.5$ both the thermal and concentration layers have maximum fall near the plate. It is due to the fact that interplay of magnetic parameter and drag force both cause a decrease in the temperature and concentration.

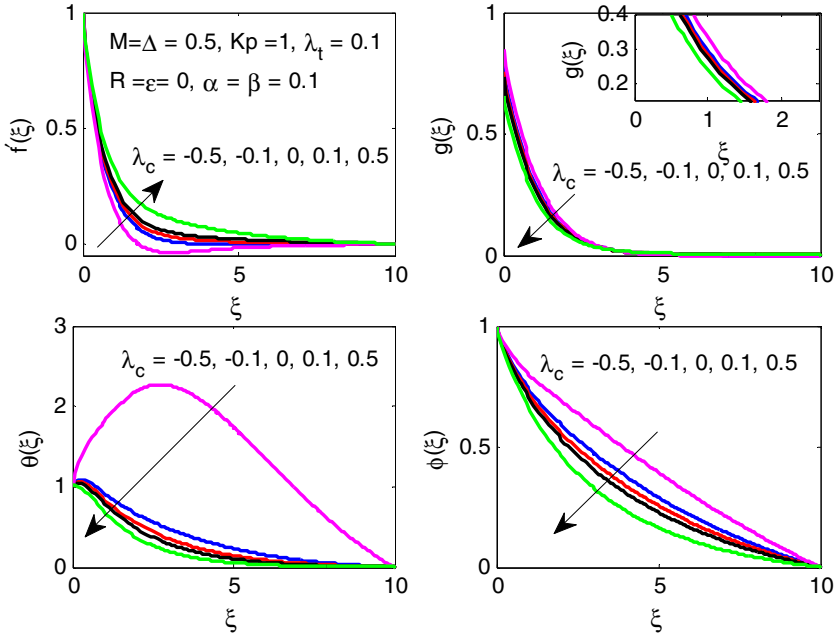


**Fig. 5.** Effect of $\lambda_c$ on velocity, microrotation, temperature and concentration profiles.

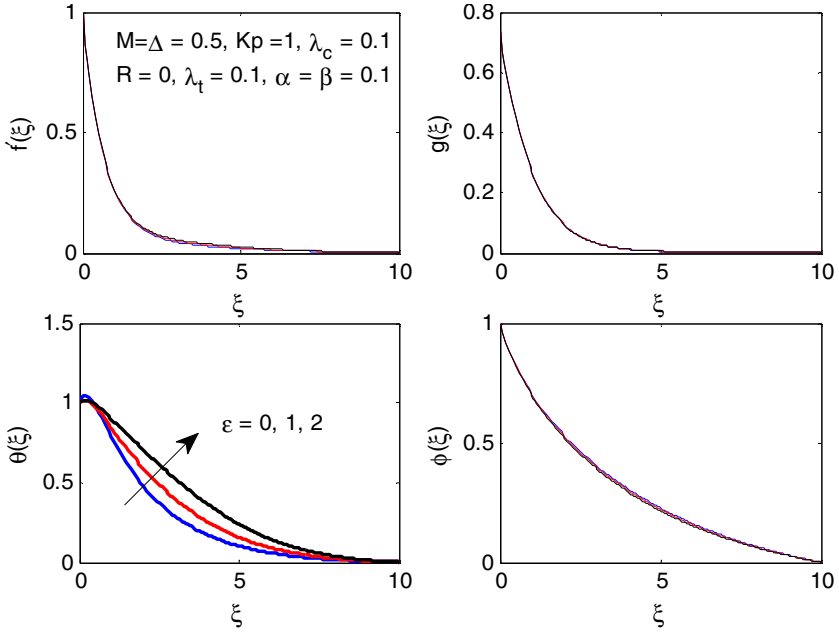


**Fig. 6.** Effect of $\varepsilon$ on velocity, microrotation, temperature and concentration profiles.

The variation of solutal buoyancy on the velocity, microrotation, temperature and concentration are well exhibited in Fig. 5. It is observed that the velocity profile increases with an increase in solutal buoyancy whereas the microrotation, thermal and concentration boundary layers decreases. It is interesting to report that for $\lambda_c = -0.5$ the thermal boundary layer enhances drastically cause a maximum temperature at the middle of the boundary layer. It is due to the fact that the presence of source/temperature dependent parameter $\alpha$ and $\beta$ contribute significantly to increase the temperature in all the layers.

The contribution of radiation parameter on temperature profile is depicted in Fig. 7 with the presence/absence of the surface condition parameter. It is evident from the boundary condition, $N = -s\frac{\partial u}{\partial y}$, that $s = 0$ implies there is no microrotation. It is seen that temperature increases with an increase in thermal radiation under the influence of surface condition parameter i.e. for both the absence of $s$ ($s = 0$) and presence of $s$ ($s = 1$).

Figs. 8 and 9 exhibit the effect of source/temperature dependent parameter on temperature profile in the absence/presence of surface condition parameter. From Fig. 8 it is remarked that the temperature profile has pick near the plate and then decreases gradually to meet the boundary condition whereas from Fig. 9 it is seen that temperature profile is asymptotic in nature. But the temperature increases significantly throughout the boundary layer

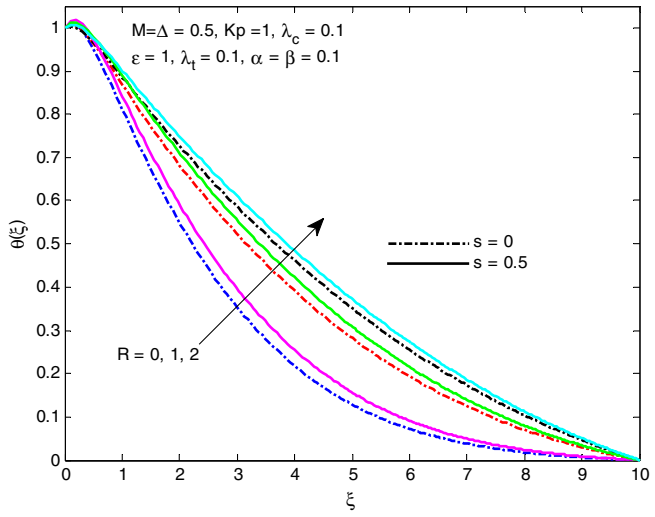


**Fig. 7.** Effect of radiation on temperature profiles.

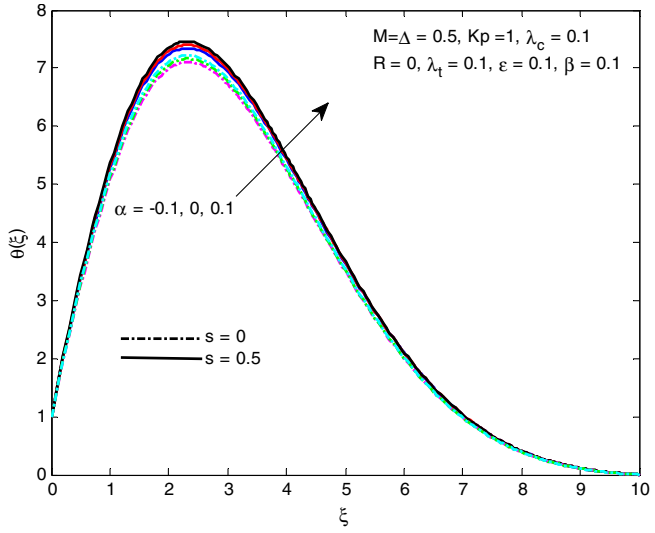


**Fig. 8.** Effect of $\alpha$ on temperature profiles.

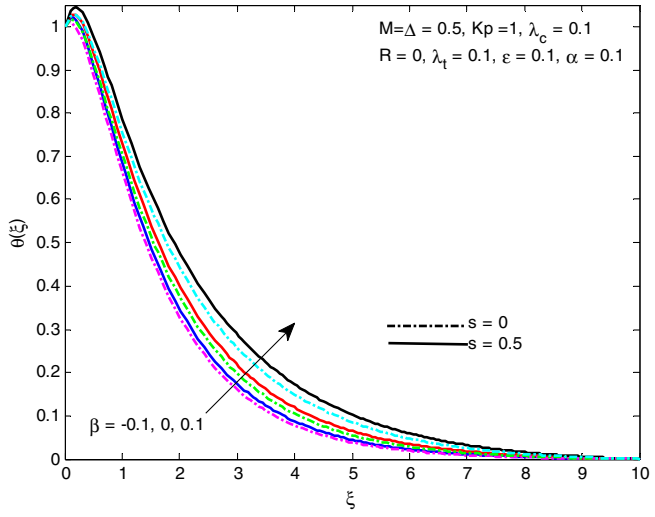


**Fig. 9.** Effect of $\beta$ on temperature profiles.

in both the presence/absence of surface condition parameter. Thus, it is concluded that the higher shear rate in the presence of source/temperature dependent parameter $\alpha$ and $\beta$ contribute significantly to increase the temperature in all the layers.

Fig. 10 depicts the effect of Soret on concentration profile for both the absence/presence of surface condition parameter. It exhibits a dual character in the concentration boundary layer and observed that increase in Soret number decreases the concentration near the plate up to a region $\xi < 5$ and after that the effect is reversed. The effect of surface condition parameter is shown in dotted ($s = 0$) and bold ($s > 0$)lines. It is seen that the effect of surface condition parameter on the concentration boundary layer is insignificant.

Fig. 11 exhibits solutal variation and Schmidt number through concentration profiles. The negative value of $\delta(\delta < 0)$ corresponds to constructive, the positive value of $\delta(\delta > 0)$ corresponds to destructive and $(\delta = 0)$ corresponds to no chemical reaction. This shows, contribution of chemical reaction as well as Schmidt number is significant in reducing the concentration distribution but on careful observation, it is seen that for higher value of Schmidt number $Sc = 0.78$, concentration distribution is not affected significantly (coincidence of curves), irrespective of constructive or

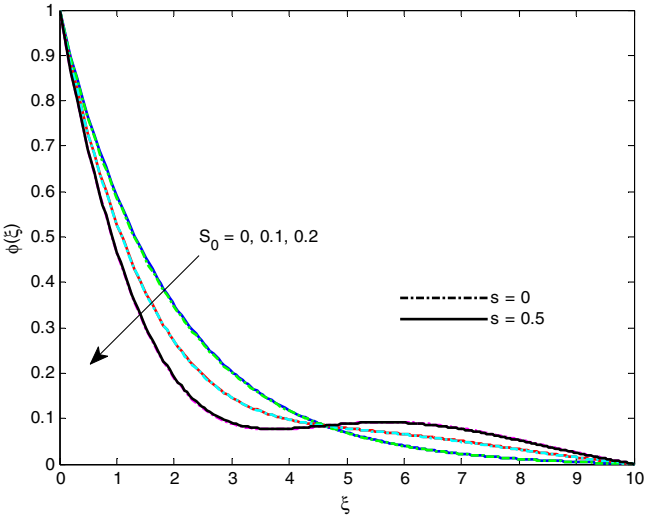


**Fig. 10.** Effect of $S_0$ on concentration profiles.

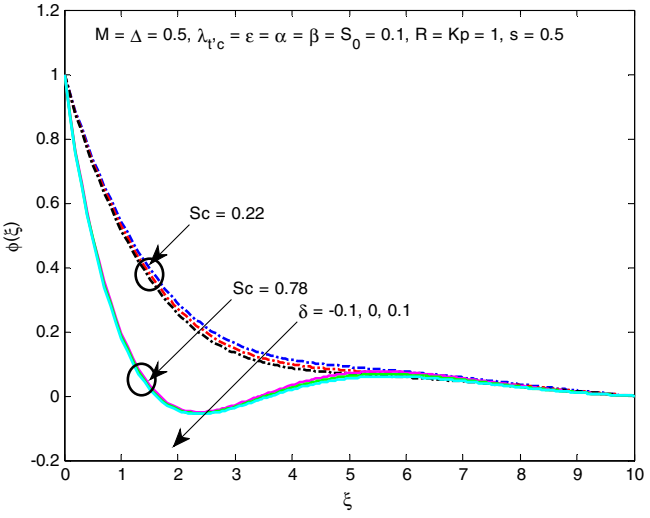


**Fig. 11.** Effect of Schmidt number and chemical reaction on concentration profiles.

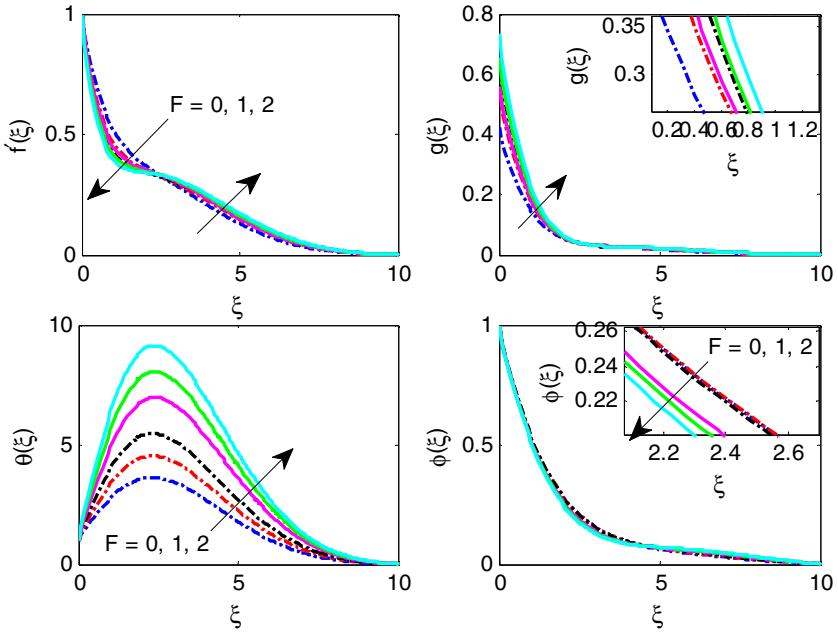


**Fig. 12.** Effect of drag coefficient on velocity, microrotation, temperature and concentration profiles.

destructive chemical reaction. To sum up, heavier species (higher value of *Sc*) and chemical reaction coefficient reduce the solutal boundary layer thickness.

Fig. 12 illustrates the inertia coefficient on the velocity, microrotation, temperature and concentration profiles in the presence of other pertinent physical parameters. It is remarked that sharp fall of velocity in the velocity boundary layer as inertia coefficient increases up to a region $\xi < 2.5$ and then reverse trend occurs to meet the boundary conditions. It is due to the fact that, inclusion of Lorentz force which is a resistive force; produces electromagnetic origin in the presence of porous matrix retards the profile. Further, microrotation profile increases with the increase in inertia coefficient. From the figure it is clear to note that the fluid temperature increases significantly with the increase in inertia coefficient in both the absence/presence of surface condition parameter. It is observed that the higher shear rate i.e. higher value of $s$, ($s = 2$) (bold lines) in the presence of source/temperature dependent parameter $\alpha$ and $\beta$ contribute significantly to increase the temperature in all the layers. The effect of inertia coefficient on the concentration profile is insignificant but the profile decreases slightly.

The rate of shear stress is calculated and the coefficient of local skin friction for different values of material parameter in the absence of other parameters is computed and presented in Table 1. The present result is compared with the earlier published results of Qasim et al. [23] and Kumar [38] and concluded that the present result is in good agreement with previous works. Table 2 presents the comparison of rate of heat transfer with the results of Grubka and Bobba [7], Chen and Char [6], Ishak et al. [19] and Kumar [38] for different values of Prandtl number in the absence of other parameters.

**Table 1**
Comparison of $\mathrm{Re}_x^{1/2} C_f$ for different values of $K$ with all other parameters are zero.

| $K$ | Qasim et al.[23] | Kumar [38] | Present solution |
|---|---|---|---|
| 0 | −1.000000 | −1.000008 | −1.0000082 |
| 1 | −1.367872 | −1.367996 | −1.3679963 |
| 2 | −1.621225 | −1.621575 | −1.6215752 |
| 3 | – | −1.827392 | −1.8273822 |
| 4 | −2.004133 | −2.005420 | −2.0054204 |

**Table 2**
Comparison of $-\theta'(0)$ for different values of Pr with all other parameters is zero.

| $K$ | Grubka and Bobba [7] | Chen and Char [6] | Ishak et al. [19] | Kumar [38] | Present |
|---|---|---|---|---|---|
| 1 | 1.3333 | 1.33334 | 1.3333 | 1.33333334 | 1.3333325 |
| 3 | 2.5097 | 2.50997 | 2.5097 | 2.50972157 | 2.50971224 |
| 10 | 4.7969 | 4.79686 | 4.7969 | 4.79687059 | 4.7968048 |

**Table 3**
Skin friction coefficient, rate of heat transfer and mass transfer.

| | | | | | | | | | |
|---|---|---|---|---|---|---|---|---|---|
| 0 | 0.2 | 0.2 | 0.3 | 0.1 | 0.1 | 0.1 | −1.0526 | 1.068862 | 0.514695 |
| 0.5 | 0.2 | 0.2 | 0.3 | 0.1 | 0.1 | 0.1 | −0.89089 | 1.093242 | 0.536834 |
| 0.5 | 1 | 0.2 | 0.3 | 0.1 | 0.1 | 0.1 | −1.15137 | 1.003129 | 0.490326 |
| 0.5 | 0.2 | 0.4 | 0.3 | 0.1 | 0.1 | 0.1 | −0.92645 | 1.085308 | 0.532187 |
| 0.5 | 0.2 | 0.2 | 1 | 0.1 | 0.1 | 0.1 | −0.88557 | 0.857909 | 0.543838 |
| 0.5 | 0.2 | 0.2 | 0.3 | 0.2 | 0.1 | 0.1 | −0.89056 | 1.064909 | 0.537505 |
| 0.5 | 0.2 | 0.2 | 0.3 | 0.1 | 0.4 | 0.1 | −0.88941 | 0.982352 | 0.539531 |
| 0.5 | 0.2 | 0.2 | 0.3 | 0.1 | 0.1 | 0.5 | −0.88879 | 1.09432 | 0.466464 |

Table 3 presents the coefficient of skin friction, rate of heat transfer at the surface and rate of mass transfer in the presence of various pertinent parameters. It is seen that the parameters $\Delta, s, R, Ec$ and $S_0$ decreases the coefficient of skin friction whereas $M$ and $\varepsilon$ enhance it significantly in magnitude. The rate of heat transfer at the surface there by cooling of the surface can be accelerated more effectively by increasing

$\Delta, s, \varepsilon$ and $S_0$. It is also observed that rate of heat transfer decreases with the increase in the values of the parameters $M, Ec$ and $R$. It is also clear to note that parameters $M, \varepsilon$ and $S_0$ reduce the rate of mass transfer at the plate whereas increasing $\Delta, s, R$ and $Ec$ parameter enhances the solutal concentration at the plate.

## 6. Conclusions

The numerical investigation has been carried out in the present study to analyze the influence of governing over a stretching sheet

embedded in a porous medium in the presence of thermal and solutal buoyancy parameters, non-uniform heat source, first order chemical reaction and Soret number. The governing partial differential equations are formulated into ordinary differential equations with the help of similarity transformation and variables. And being solved numerically by using Runge–Kutta method with shooting technique. We have acquired interesting observations graphically for these pertinent parameters which are summarized below:

(1) The velocity profile reduces due to increase in magnetic parameter in both the presence/absence of porous matrix.
(2) The effect of porosity of the medium combined with inertia effect gives rise to a transverse compression producing a thinner boundary layer.
(3) For microrotation in the presence of inertia coefficient and porosity of the medium flow reversal occur.
(4) Higher values of surface condition parameter and porosity of the medium contribute to enhance the microrotation and absence of the effect of these parameters leads to linearise the variation of microrotation profile. Higher share rate and viscous dissipation contribute to growth of thermal boundary layer.
(5) Thermal buoyancy enhance the velocity distributions significantly whereas flow instability occurs for higher value of heating of the plate i.e. $\lambda_t = -0.5$.
(6) The fluid temperature increases with the increase in inertia coefficient in both the absence/presence of surface condition parameter.
(7) Heavier species, chemical reaction coefficient and magnetic field reduce the solutal boundary layer.
(8) Increase in magnetic parameter, porous matrix and inertial effect increases the skin friction while it decreases with increase in material parameter.
(9) Increase in magnetic parameter, porous matrix and inertial effect Sherwood number decreases whereas it increases with an increase in material parameter, Schmidt number and chemical reaction parameter.

It is hoped that present investigation will provide an useful information for many scientific and industrial applications and also serve as a complement to the previous studies.

## References


[1] R. Bhargava, H.S. Takhar, Numerical study of heat transfer characteristics of the micropolar boundary layer near a stagnation point on a moving wall, Int. J. Eng. Sci. 38 (2000) 383–394.
[2] Nisat Nowroz Anika, Md. Mainul Hoque, S. Hossain, Md. Mahmud Alam, Thermal diffusion effect on unsteady viscous MHD micropolar fluid flow through an infinite plate with hall and ion-slip current, Proc. Eng. 105 (2015) 160–166.
[3] A.C. Eringen, Theory of micropolar fluids, J. Math. Mech. 16 (1964) 1–18.
[4] B.C. Sakiadis, Boundary layer behavior on continuous solid surfaces: the boundary layer on a continuous flat surface, AIChE J. 7 (1961) 221–225.
[5] Y.J. Kim, J.C. Lee, Analytical studies on MHD oscillatory flow of a micropolar fluid over a vertical porous plate, Surf. Coat. Technol. 171 (2003) 187–193.
[6] C.K. Chen, M.I. Char, Heat transfer on continuous stretching surface with suction or blowing, J. Math. Anal. Appl. 135 (1988) 568–580.
[7] L.G. Grubka, K.M. Bobba, Heat transfer characteristics of a continuous stretching surface with variable temperature, ASME J. Heat Transfer 107 (1985) 248–250.
[8] S. Baag, S.R. Mishra, G.C. Dash, M.R. Acharya, Numerical investigation on MHD micropolar fluid flow toward a stagnation point on a vertical surface with heat source and chemical reaction, J. King Saud Eng. Sci. (2014), http://dx.doi.org/10.1016/j.jksues.2014.06.002.
[9] Md. Mainul Hoque, Md. Mahmud Alam, M. Ferdows, O. Anwer Beg, Numerical simulation of dean number and curvature effects on magneto-bio-fluid flow through a curved conduit, Proc. Inst. Mech. Eng. Part H J. Eng. Med. 227 (11) (2013) 1155–1170.
[10] O. Anwer Beg, Md. Mainul Hoque, M. Wahiduzzaman, Md. Mahmud Alam, M. Ferdows, Spectral numerical simulation of mageneto-physiological laminar dean flow, J. Mech. Med. Biol. 14 (4) (2014). ID-1450047.
[11] Md. Mainul Hoque, Md. Mahmud Alam, A numerical study of MHD laminar flow in a rotating curved pipe with circular cross section, Open J. Fluid Dyn. 5 (2015) 121–127.
[12] Md. Mainul Hoque, Nisat Nowroz Anika, Md. Mahmud Alam, Magnetic Effects on Direct Numerical Solution of Fluid Flow through a Curved Pipe with Circular Cross Section, Eur. J. Sci. Res. 103 (3) (2013) 343–361.
[13] N.S. Akbar, Z. Khan, S. Nadeem, W. Khan, Double-diffusive natural convective boundary-layer flow of a nanofluid over a stretching sheet with magnetic field, Int. J. Numer. Meth. Heat Fluid Flow 26 (1) (2016) 108–121.
[14] N.S. Akbar, Z. Khan, Magnetic field analysis in a suspension of gyrotactic microorganisms and nanoparticles over a stretching surface, J. Magn. Magn. Mater. 410 (2016) 72–80.
[15] L.J. Crane, Flow past a stretching plate, J. Appl. Math. Phys., (ZAMP) 21 (1970) 645–647.
[16] P.D. McCormack, L.J. Crane, Physical Fluid Dynamics, Academic Press, New York, 1973.
[17] B. Mohanty, S.R. Mishra, H.B. Pattnaik, Numerical investigation on heat and mass transfer effect of micropolar fluid over a stretching sheet, Alexandria Eng. J. 54 (2) (2015) 223–232.
[18] S.R. Mishra, G.C. Dash, P.K. Pattnaik, Flow of heat and mass transfer on MHD free convection in a micropolar fluid with heat source, Alexandria Eng. J. 54 (3) (2015) 681–689.
[19] A. Ishak, R. Nazar, I. Pop, Hydromagnetic flow and heat transfer adjacent to a stretching vertical sheet, Heat Mass Transf. 44 (2008) 921–927.
[20] R. Mehmood, S. Nadeem, N.S. Akbar, Oblique stagnation flow of Jeffery fluid over a stretching convective surface: optimal solution, Int. J. Numer. Meth. Heat Fluid Flow 25 (3) (2015) 454–471.
[21] N.S. Akbar, A. Ebaid, Z. Khan, Numerical analysis of magnetic field on Eyring-Powell fluid flow towards a stretching sheet, J. Magn. Magn. Mater. 382 (2015) 355–358.
[22] M.S. Abel, P.G. Siddheshwar, M.M. Nandeppanavar, Heat transfer in a viscoelastic boundary layer flow over a stretching sheet with viscous dissipation and non-uniform heat source, Int. J. Heat Mass Transfer 50 (2007) 960–966.
[23] M. Qasim, I. Khan, S. Shafie, Heat transfer in a micropolar fluid over a stretching sheet with Newtonian heating, PLoS ONE 8 (2013) e59393.
[24] D. Pal, H. Mondal, Effect of variable viscosity on MHD non-Darcy mixed convection heat transfer over a stretching sheet embedded in a porous medium with non-uniform heat source/sink, Commun. Nonlinear Sci. Numer. Simul. 15 (2010) 1533–1564.
[25] D. Bhukta, G.C. Dash, S.R. Mishra, Heat and mass transfer on MHD flow of a viscoelastic fluid through porous media over a shrinking sheet, Int. Sch. Res. Notices 2014 (2014). Article ID 572162, 11 pages.
[26] S. Nadeem, R. Mehmood, R. Noreen, Non-orthogonal stagnation point flow of a nano non-Newtonian fluid towards a stretching surface with heat transfer, Int. J. Heat Mass Transfer 57 (2013) 679–689.
[27] T. Hayat, S. Asad, M. Qasim, Hendi, Boundary layer flow of a Jeffery fluid with convective bf boundary conditions, Int. J. Numer. Methods Fluids 69 (2012) 1350–1362.
[28] R. Haq, S. Nadeem, N.S. Akbar, Z. Khan, Radiation effect on stagnation point flow of micropolar nanofluid along a vertically convective stretching surface, IEEE Trans. Nanotechnol. 14 (2015) 42–50.
[29] S. Baag, M.R. Acharya, G.C. Dash, S.R. Mishra, MHD flow of a visco-elastic fluid through a porous medium between infinite parallel plates with time dependent suction, J. Hydrodyn. 27 (5) (2015) 840–847.
[30] C.S.K. Raju, N. Sandeep, V. Sugunamma, M. Jayachandra Babu, J.V. Ramana Reddy, Heat and mass transfer in magnetohydrodynamic Casson fluid over an exponentially permeable stretching surface, Eng. Sci. Technol. Int. J. 19 (1) (2016) 45–52.
[31] N. Sandeep, C. Sulochana, B. Rushi Kumar, Unsteady MHD radiative flow and heat transfer of a dusty nanofluid over an exponentially stretching surface, Eng. Sci. Technol. Int. J. 19 (1) (2016) 227–240.
[32] R.S. Tripathy, G.C. Dash, S.R. Mishra, S. Baag, Chemical reaction effect on MHD free convective surface over a moving vertical plane through porous medium, Alexandria Eng. J. 54 (3) (2015) 673–679.
[33] T. Hayat, H. Yasmin, S. Asghar, A.A. Hendi, Slip effects on peristaltic transport in an inclined asymmetric channel with mass transfer and chemical reaction, Appl. Bionics Biomech. 10 (1) (2013) 41–58.
[34] T. Hayat, H. Yasmin, B. Ahmad, G. Chen, Exact solution for peristaltic transport of micropolar fluid in a channel with convective boundary conditions and heat source/sink, ZNA 69 (8–9) (2014).
[35] T. Hayat, H. Yasmin, M. Al-Yami, Soret and Dufour effects in peristaltic transport of physiological fluids with chemical reaction: a mathematical analysis, in: Comput. Fluids 89 (2014) 242–253.
[36] T. Hayat, Y. Saeed, S. Asad, A. Alsaedi, Soret and Dufour effects in the flow of Williamson fluid over an unsteady stretching surface with thermal radiation, in: ZNA 70 (4) (2014).
[37] T. Hayat, S. Asad, M. Mustafa, A. Alsaedi, MHD stagnation point flow of Jeffrey fluid over a convectively heated stretching sheet, Comput. Fluids 108 (2015) 179–185.
[38] L. Kumar, Finite element analysis of combined heat and mass transfer in hydromagnetic micropolar flow along a stretching sheet, Comput. Mater. Sci. 46 (2009) 841–848.

[39] M. Muskat, Flow of Homogeneous Fluid through Porous Media, McGraw-Hill, New York, 1937.
[40] R.E. Collins, Flow of Fluids through Porous Materials, Reinhold Publishing Corp., New York, 1961.
[41] J. Bear, Dynamics of Fluids in Porous Media, American Elsevier pub. Co., New York, 1972.
[42] D.A.S. Rees, I. Pop, IMA J. Appl. Math. 61 (1998) 179–197.
[43] Emad M. Abo-Eldahab, Mohamed A. El Aziz, Flowing/suction effect on hydromagnetic heat transfer by mixed convection from an indicated continuously stretching surface with internal heat generation/absorption, Int. J. Therm. Sci. 43 (2004) 709–719.